JMEPEG (2007) 16:601–606
DOI: 10.1007/s11665-007-9042-2

1059-9495/$19.00

Mechanical Properties and Fracture Surface Morphologies in Unnotched Specimens of Rubber-PMMA Composites

Shiyun Gong and Sri Bandyopadhyay

(Submitted April 13, 2006; in revised form June 6, 2006)

Correlations between mechanical properties and microscopic features were investigated using unnotched specimens of rubber-PMMA composites in very low to medium range of cross head speeds. It is found that: (1) a trapezoid-shaped smooth region and fish scale-like texture with bands in rough region correlates with brittle failure in pure PMMA, while a quarter circle-shaped smooth region and hackle-like texture, and the presence of dimples and/or voids correlate with ductile failure in rubber-PMMA composites; (2) decrease in degree of roughness in rubber-PMMA composites can be correlated with decrease in Young's modulus; (3) decrease in size of the smooth region with increasing speed can be correlated with decrease in modulus of toughness; (4) larger smooth region in rubber-PMMA composites containing more rubber correlates with higher modulus of toughness.

Keywords blends, electron microscopy, fractography, fracture toughness, mechanical properties, rubber-PMMA composites

1. Introduction

Toughened polymers, in the form of co-polymers or blends, are very important materials consisting of a high modulus phase with modulus of elasticity (E) typically 3 GPa, and a low modulus rubbery phase with E of the order of a few to several MPa. The deformation mechanisms of toughened polymers have been extensively studied in the literature but not yet properly understood because the base thermoplastic or thermoset polymers can undergo plastic deformation by mixed modes of shear yielding and crazing (Ref 1-3). The addition of a soft phase can add or induce more complexity in the deformation behavior of toughened polymers either as an inclusion, an interface or interphase, raiser of triaxiality, a bridge-forming element or by its own deformation modality. Examples of conventional unnotched testing as a function of strain rate and temperature (Ref 4-6) as well as fracture mechanics-based notched specimen testing under pseudo-static and impact rates (Ref 7) are available in the literature. In recent work, ductile-brittle transition and dynamic fracture studies have been employed in toughened glassy polymers (Ref 8-10), whereas micromechanical studies and ultrasonic measurements undertaken in toughened glassy polymers, semicrystalline polymers or polymer matrix composites (Ref 11-13) have yielded useful information. In addition, more recent studies concerning crack velocity and corresponding fracture surfaces (Ref 14-16), stress concentration at notch tip (Ref 17), and morphologies in different part of the fracture surface (Ref 18) give us a good understanding of deformation and fracture mechanisms.

However, some aspects or problems in the field have not been explored adequately and systematically. Here are some examples. It is known that toughened plastics are viscoelastic in nature (Ref 19-22), and test speed has a significant effect on test results; however, medium-to-high test speeds have generally been employed in the literature mostly because these tests are less time-consuming (hence less expensive) and this has left a significant gap in data in the lower range of test speeds. Second, it is known that a notch can markedly reduce fracture stress of a brittle glassy polymer like poly(methyl methacrylate) (PMMA) and make ductile materials like rubber-toughened PMMA (RTPMMA) fail in a brittle manner (Ref 23); however, it is little known how the difference in the fracture surface morphologies for the two modes of fracture looks like.

The present authors take the view that study of toughened polymers should be investigated from a broader point of view. This means not only that both conventional unnotched and fracture mechanics-based notched tests need to be carried out experimentally on the same materials under identical test conditions to get comparative and meaningful results, but also that extensive scanning and transmission electron microscopic studies need to be carried out systematically in later stage to obtain correlations between macroscopic mechanical properties and microscopic features on fracture surfaces of test specimens to identify and support/complement findings of mechanical test results and get a global understanding of the findings.

This research studies commercial grades of toughened polymers as these are the ones available in the open market for use in actual engineering applications. Moreover, the research employs slow-to-medium test speeds to fill a significant gap in data in the lower range of test speeds. Particularly, the research devotes attention to the microscopic examination

Shiyun Gong, College of Materials Science and Engineering, Harbin University of Science and Technology, Harbin 150040, China. Contact e-mail: shiyun@yahoo.com. **Sri Bandyopadhyay,** School of Materials Science and Engineering, University of New South Wales, Sydney 2052, Australia.

of deformation/fracture features, in an attempt to reveal correlations between macroscopic properties and microscopic features.

This article, part I presents the results using only unnotched specimens.

2. Experimental

2.1 Materials

Main test materials selected for the program are two commercial grades of RTPMMA from Cadillac Plastics Sydney, Australia—5xPMMA and 8xPMMA significantly differing in rubber content, termed as RTPMMA-1 and RTPMMA-2, respectively. An untoughened (pure) PMMA obtained from the same commercial source is also studied in parallel as a control material against which RTPMMA-1 and RTPMMA-2 are compared. Cast sheets of the three investigated materials were purchased; however, materials information was not released. Therefore, we determined experimentally on our own the materials information such as rubber particle structure and rubber content, using characterization methods such as transmission electron microscopy(TEM) examination and calculations based on the rule of mixtures (Ref 24). Details of the materials are given in Table 1.

2.2 Experimental Program

Unnotched specimens were machine-cut from the cast sheets in accordance with ASTM D 638 Type I (specified gauge length 50 mm), and left at room temperature 19 °C for at least 48 h before being tested.

The tests were conducted in an Instron Model 1185 Testing Machine, at cross head speeds (CHS): 0.05, 0.5, 1, 5, and 10 mm/min. Logarithmic values of CHSs and their corresponding strain rates are given in Table 2, where strain rate is obtained by dividing CHS by gauge length, i.e., 50 mm and then changing to s^{-1}.

The load and the cross-head displacement were recorded on a strip chart recorder. Cross head and chart speed were set at 1:1. The full scale load was set at 5 kN for PMMA, and 2 kN for RTPMMA-1 and RTPMMA-2. For measuring modulus of elasticity, an Instron strain gauge extensometer (type 2630-015, gauge length 25 mm) was used with 1000× magnification of deflection.

Specimens for scanning electron microscopy (SEM) and field emission SEM(FESEM) examinations of fracture surface were saw-cut from fractured test specimens, about 5 mm below fracture surface, mounted on aluminum stubs (ø25 mm × 5 mm) after cleaning, and then coated with gold in a JEOL JEE-400 Vacuum Evaporator.

Table 2 Logarithmic values of CHSs and their corresponding strain rates

CHS, mm/min	0.05	0.5	1	5	10
lnCHS	−3	−0.69	0	1.61	2.30
$\dot{e}$, s^{-1}	1.67×10^{-5}	1.67×10^{-4}	3.33×10^{-4}	1.67×10^{-3}	3.33×10^{-3}
ln $\dot{e}$	−11	−8.7	−8	−6.4	−5.7

Scanning electron microscopy examination of gold-coated fracture surfaces were performed in a JEOL LXA-840 Scanning Microanalyzer for low magnifications (lower than 3k), and FESEM examination a HITACHI S-4500 Scanning Electron Microscope for high magnifications (×5k or ×l0k). To prevent fracture surface from being damaged during examination, low accelerating voltages were used. The satisfactory result was obtained by using accelerating voltages of 5 kV for SEM and 1 kV for FESEM.

3. Results and Discussion

3.1 Mechanical Properties

In the tensile testing, pure PMMA failed in a brittle manner, while RTPMMA-1 and RTPMMA-2 failed in a ductile one, as shown in Fig. 1. Test results of Young's modulus E, yield stress σ_y, yield strain ε_y, and fracture strain ε_f are summarized in Table 3 and discussed as follows.

It is seen in Table 3 that: (1) E increases by about 20% within the speed range, while decreases by about 40% after toughening; (2) pure PMMA has the highest value of E; RTPMMA-2 has the lowest one and RTPMMA-1 is in the middle. The incorporation of rubber in PMMA is responsible for a reduction in E, and the more rubber in RTPMMA, the more is the reduction. An increase in E with increasing CHS is due to viscoelasticity of polymer.

It is also seen in Table 3 that: (1) both yield stress and yield elongation are rate dependent; yield stress increases as CHS increased and in contrast, yield elongation decreases as CHS increased; a linear relationship between yield stress and ln(strain rate) indicates the presence of Eyring volume associated with activated yielding in the RTPMMA polymers (Ref 25); (2) RTPMMA material containing less rubber, i.e., RTPMMA-1, has higher yield stress and lower elongation; (3) fracture strain ε_f is 4 to 5 times higher than yield strain ε_y.

Lastly, fracture strain values in Table 3 show that: (1) greatly enhanced extension is achieved by the incorporation of rubber in PMMA; the more the rubber, the greater the extension: about 7-fold extension for RTPMMA-1 and about

Table 1 Test materials and their physical characteristics

Testing material & nature	Thickness of sheet, mm	Rubber particle structure, from TEM exam.	Content of rubber particles, vol.%, from TEM exam.	Content of rubber, vol.%, from rule of mixtures	T_g, glass trans temp, from DSC test, °C
Pure PMMA, transparent	4	Not applicable	0	0	117
5xRTPMMA(RTPMMA-1), transparent, 5 times more ductile than pure PMMA	3	Hard core-soft shell (three layer particles)	17.8	13.8	111
8xRTPMMA(RTPMMA-2), transparent, 8 times more ductile than pure PMMA	3	Hard core-soft shell (three layer particles)	41.9	41.4	110

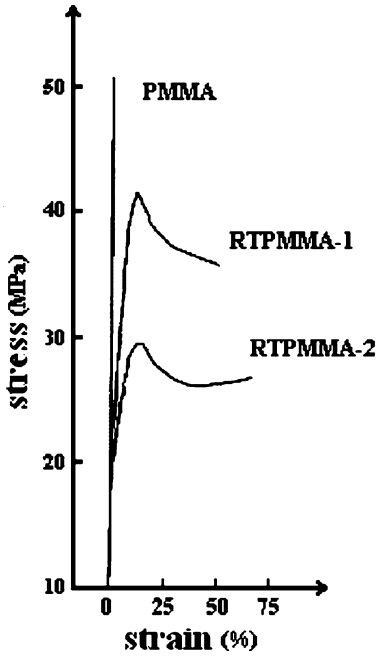

Fig. 1 Experimental stress-strain curves at CHS 0.5 mm/min of three investigated materials

Table 3 Average valves of E(GPa), σ_y (MPa), σ_f (MPa), ε_y (%), and ε_f (%) in three materials

		CHS, mm/min				
Material		**0.05**	**0.5**	**1**	**5**	**10**
Pure PMMA	E	2.9	3.0	3.1	3.5	3.4
	σ_f	46.1	51.4	52.5	57.4	61.0
	ε_f	5.60	5.46	4.67	4.60	4.80
RTPMMA-1	E	2.5	2.6	2.6	2.8	3.1
	σ_y	42.4	50.0	51.4	55.8	59.8
	ε_y	10.0	9.2	9.0	9.0	8.2
	ε_f	49.18	41.66	39.87	36.67	33.46
RTPMMA-2	E	1.7	2.0	2.2	2.2	2.3
	σ_y	31.3	35.7	38.8	42.8	44.5
	ε_y	15.4	13.2	12.0	11.2	11.2
	ε_f	72*	59.66	54.87	48.60	47.34

* Not fail after 6 h of tension

10-fold extension for RTPMMA-2 at high end of CHS range were reached; (2) speed has great effect on extension in RTPMMA especially at low end of CHS range; the lower the CHS, the greater the extension. Specimens of RTPMMA-2 did not break after 6 h of tension at CHS 0.05 mm/min and the strain at that moment was 72%.

Based on data in Table 3, modulus of toughness, T for the RTPMMA materials can be worked out, using equation $T = \sigma_u \cdot \varepsilon_f$ (Ref 26). The T data are plotted v. ln (strain rate) in Fig. 2.

It is noted that about 10-fold increase in energy absorption can be achieved after toughening PMMA. This is a practically realistic estimate of toughening. In addition, Fig. 2 also shows that: (a) RTPMMA-2 containing more rubber is higher in T; however, a small T rise between RTPMMA-2 and RTPMMA-1

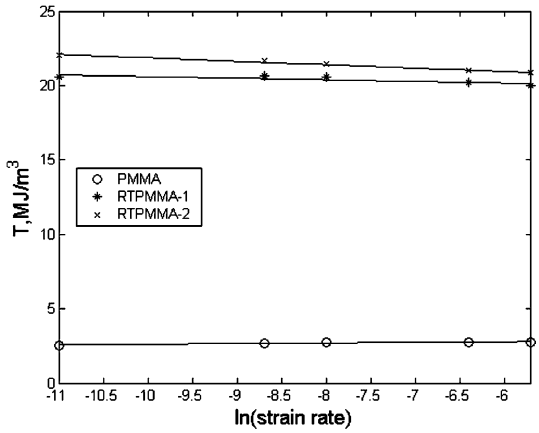

Fig. 2 T versus natural logarithm of strain rate

suggests that T is not in proportion with their rubber contents; (b) graphs for RTPMMA have a slightly negative slope; total energy for RTPMMA decreases slightly as strain rate is increased, indicating viscoelastic effect.

3.2 Fracture Surface Morphologies

(1) Low magnification surface morphologies

Low magnification SEM fracture surfaces of pure PMMA, RTPMMA-1 and RTPMMA-2 at two extreme ends of the CHS range, i.e., 0.05 and 10 mm/min, are presented in Fig. 3.

Figure 3 shows, in terms of surface roughness, three regions—a smooth region, a rough region, and a transition region, i.e., border between the smooth and rough regions, and surface texture variation with grade of material. Main surface features are represented schematically in Fig. 4, and a brief description of the features is given as follows.

Of the three regions as shown in Fig. 4, rough region dominates the fracture surface of each material and its degree of coarseness goes down in the three materials system—pure PMMA has the most rampant form of crack propagation, while RTPMMA-2 containing more rubber has the least rampant form of crack propagation. Moreover, a major difference in texture exists between pure PMMA and RTPMMA—pure PMMA exhibits fish scale-like texture, while RTPMMA exhibits hackle or ray-like texture. It can be noted that degree of coarseness and surface texture in rough region vary with rubber content; and more rubber yields a less tortuous texture in rough region.

Smooth region, which represents initiation region, i.e., slow, stable, sub-critical crack growth, is most important in terms of stable crack propagation. Smooth regions have different shapes between pure PMMA and RTPMMA, and their size varies with CHS as seen in Fig. 3. RTPMMA has a smooth region of about a quarter of circular area, while pure PMMA exhibits a kind of trapezoid area. If the border between the smooth and rough regions is viewed as a part of an arc, the arc center for RTPMMA might be close to or coincide on one of the corners of specimen cross-section, while the one for pure PMMA not. Size or length of smooth regions was measured, taking mean radius of circular area as length for smooth region in RTPMMA and mean distance to first band on crack path as length for smooth region in pure PMMA. Measured values in mm are presented in Table 4. It is seen that: (1) the smooth region in RTPMMA-2 is larger than that in RTPMMA-1, as a whole; and

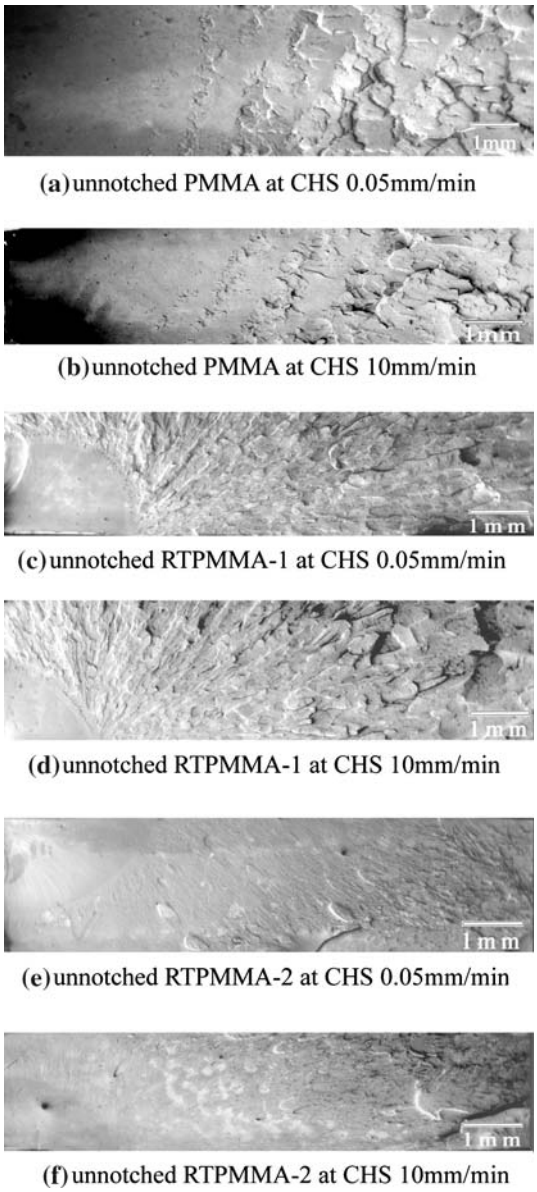

Fig. 3 SEM micrographs showing three regions and other features on fracture surfaces in the materials (fracture origin on the left of micrographs)

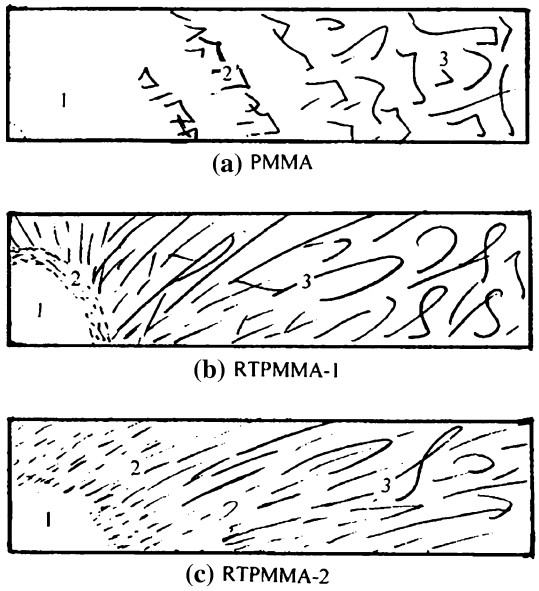

Fig. 4 Schematic representation of fracture surfaces in the materials (1—smooth region, i.e., stable, slow, sub-critical growth; 2—transition region; 3—rough region, i.e., fast crack propagation)

Table 4 Average length values of smooth regions in mm

	CHS, mm/min				
Material	**0.05**	**0.5**	**1**	**5**	**10**
Pure PMMA	5.25	4.91	4.95	4.73	4.40
RTPMMA-1	2.53	2.23	2.01	1.79	1.72
RTPMMA-2	2.51	2.24	2.18	2.21	2.21

(2) pure PMMA has the largest smooth region; however, the region sizes for pure PMMA and RTPMMA might not be comparable with each other because mechanisms for formation of the different shapes might be different.

Transition region is found to have different textures in the three materials. Pure PMMA has a transition region, which is occupied by several inclined bands. The bands become wider along crack path, while band spacing appears to be constant. Interestingly, if we take a broader view, the rough region for pure PMMA might be actually regarded as last band with greatest width on crack path. The highly discontinuous transition from slow to fast propagation in pure PMMA reflects crack velocity oscillation with increasing crack length (Ref 14, 15). By contrast, the transition region for RTPMMA-1 is confined and narrow, appearing like a sand ridge near the seashore to define a smooth region having about a quarter of circular area, while the one for RTPMMA-2 is diffuse and broad, with fine rays which extend from smooth region, grow and become hackle in rough region.

From above discussion, following correlations between mechanical properties and surface features could be revealed: (1) a trapezoid-shaped smooth region and fish scale-like texture with bands on fracture surface correlates with brittle failure in pure PMMA, while a quarter circle-shaped smooth region and hackle-like texture correlates with ductile failure in RTPMMA; (2) decrease in degree of roughness can be correlated with decrease in Young's modulus; (3) decrease in size of smooth region with increasing speed can be correlated with decrease in modulus of toughness; (4) larger smooth region in RTPMMA containing more rubber, i.e., RTPMMA-2 correlates with higher modulus of toughness and lower modulus of elasticity.

(2) Details of smooth and rough regions viewed at high magnification

Two FESEM micrographs for each fracture surface in unnotched specimens of PMMA and RTPMMA created at lowest CHS, i.e., 0.05 mm/min are presented in Fig. 5, one being from smooth region near notch tip and the other rough region.

Comparing high magnification FESEM fracture surfaces in Fig. 5, one can see that main surface feature is the surface in RTPMMA exhibits dimples and/or voids which are related to rubber particles, while the surface in pure PMMA not. Moreover, It can be noted that RTPMMA-2 containing more rubber has more dimples and/or voids than RTPMMA-1

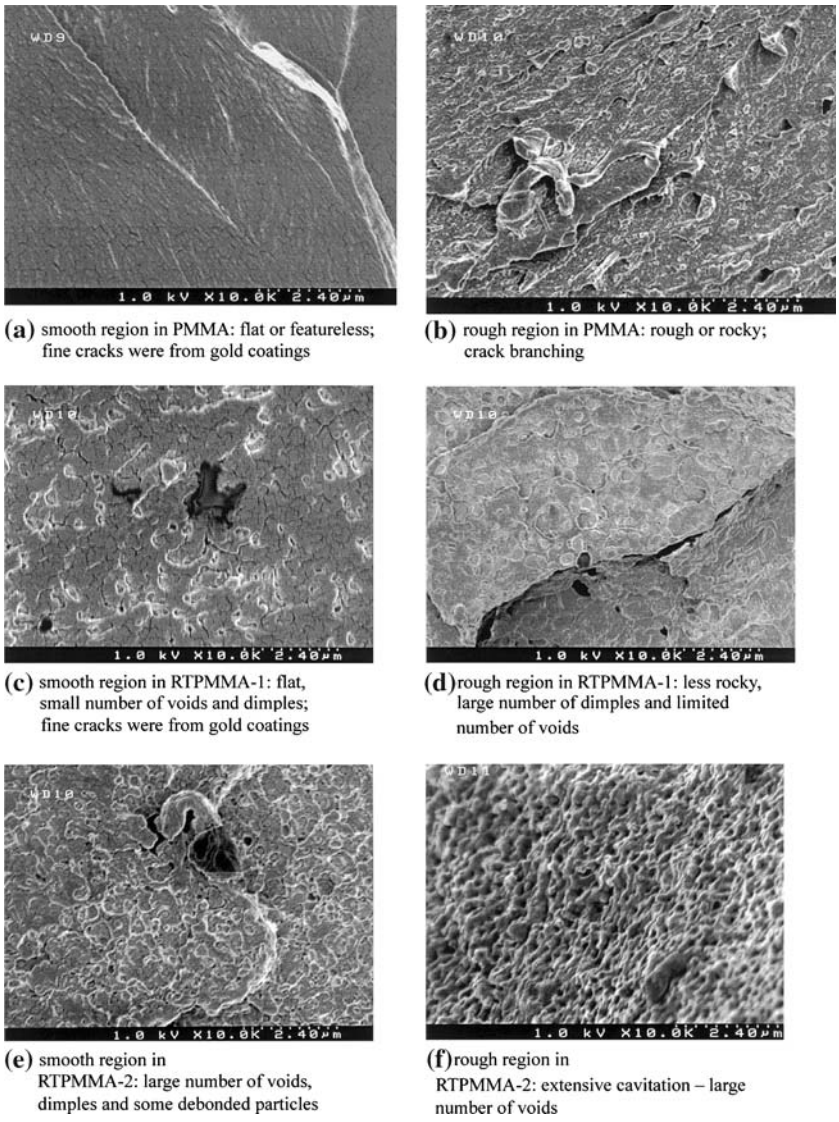

Fig. 5 FESEM micrographs showing details of smooth and rough regions in the three materials viewed at high magnification

containing less rubber. Dimples (Ref 27) might indicate debonding at particle/matrix interface and result from crack passing around debonded particles, while voids might result from cavitation of rubber particles and matrix crazing. Debonding, cavitation, and crazing may cause considerable plastic deformation and absorb a large amount of energy during tension to failure. Therefore, RTPMMA-2 exhibits the highest modulus of toughness, as shown in Fig. 2.

From the discussion, following correlations could be revealed: the presence of dimples and/or voids on surface is correlated with ductile failure, and larger number of dimples and/or voids correlates with higher value in modulus of toughness.

4. Conclusions

(1) There is a significant difference in fracture surface morphology between two modes of failure in PMMA polymers. A trapezoid-shaped smooth region and fish scale-like texture with bands in low magnification fracture surface correlates with brittle failure in pure PMMA, while a quarter circle-shaped smooth region and hackle-like texture correlates with ductile failure in RTPMMA.

(2) There is another significant difference in fracture surface morphology between two modes of failure. Ductile failure is correlated with the presence of dimples and/or voids in high magnification fracture surface, while brittle failure is correlated with the absence of dimples and/or voids; larger number of dimples and/or voids correlates with higher value in modulus of toughness

(3) Degree of roughness in RTPMMA as a whole is rubber content-dependent, and decrease in degree of roughness can be correlated with decrease in Young's modulus.

(4) Size of smooth region in the investigated materials is rate-dependent, and decrease in size of smooth region with increasing speed can be correlated with decrease in modulus of toughness.

(5) Size of smooth region in RTPMMA is rubber content-dependent, and larger smooth region in RTPMMA containing more rubber correlates with higher modulus of toughness.

References

1. C.B. Bucknall, *Toughened Plastics*. Applied Science Publishers Ltd, London, 1977
2. I.M. Ward, *Mechanical Properties of Solid Polymers*. 2nd ed., John Wiley & Sons Ltd, New York, 1990
3. S. Bandyopadhyay, Macroscopic Fracture Behaviour: Correlation with Macroscopic Aspects of Deformation in Toughened Epoxies, *Toughened Plastics I: Science & Engineering*, C. Keith Riew and Anthony J. Kinloch, Eds., Advances in Chemistry Series 233, American Chemical Society, 1993, p 211–258
4. O. Frank and J. Lehmann, Determination of Various Deformation Processes in Impact-Modified PMMA at Strain Rates up to 103 Per Minute, *Colloid Polym. Sci.*, 1986, **264**, p 473–481
5. R.W. Truss and G.A. Chadwick, The Tensile Deformation Behaviour of a Transparent ABS Polymer, *J. Mater. Sci.*, 1976, **11**, p 1385
6. R.K. Goldberg, G.D. Roberts, and A. Gilat, Incorporation of Mean Stress Effects into the Micromechanical Analysis of the High Strain Rate Response of Polymer Matrix Composites, *Compos. Part B*, 2003, **34**, p 151–165
7. C. Grein, H.-H. Kausch, and Ph. Béguelin, Characterisation of Toughened Polymers by LEFM Using an Experimental Determination of the Plastic Zone Correction, *Polymer Test.*, 2003, **22**, p 733–746
8. T. Vu-Khanh and Z. Yu, Mechanisms of Brittle-Ductile Transition in Toughened Thermoplastics, *Theor. Appl. Fract. Mech.*, 1997, **26**, p 177–183
9. W. Jiang, D. Yu, and B. Jiang, Brittle-Ductile Transition of Particle Toughened Polymers: Influence of the Matrix Properties, *Polymer*, 2002, **45**, p 6427–6430
10. Christophe FOND and Robert SCHIRRER, Dynamic Fracture Surface Energy Values and Branching Instabilities During Rapid Crack Propagation in Rubber Toughened PMMA, in C. R. Acad. Sci. Paris, t. 329, Série II b, 2001, p 195–200
11. P.A. Tzika, M.C. Boyce, and D.M. Parks, Micromechanics of Deformation in Particle-Toughened Polyamides, *J. Mech. Phys. Solids*, 2000, **48**, p 1893–1929
12. G.M. Kim and G.H. Michler, Micromechanical Deformation Processes in Toughened and Particle Filled Semicrystalline Polymers. Part 2: Model Representation for Micromechanical Deformation Processes, *Polymer*, 1998, **39**(22), p 5699–5703
13. S. Biwa, N. Ito, and N. Ohno, Elastic Properties of Rubber Particles in Toughened PMMA: Ultrasonic and Micromechanical Evaluation, *Mech. Mater.*, 2001, **33**, p 717–728
14. N. Murphy and A. Ivankovic, The Prediction of Dynamic Fracture Evolution in PMMA Using a Cohesive Zone Model, *Eng. Fract. Mech.*, 2005, **72**, p 861–875
15. X.F. Yao, W. Xu, M.Q. Xu, K. Arakawa, T. Mada, and K. Takahashi, Experimental Study of Dynamic Fracture Behavior of PMMA with Overlapping Offset-Parallel Cracks, *Polymer Test.*, 2003, **22**, p 663–670
16. F. Zhou, J.-F. Molinari, and T. Shioya, A Rate-Dependent Cohesive Model for Simulating Dynamic Crack Propagation in Brittle Materials, *Eng. Fract. Mech.*, 2005, **72**, p 1383–1410
17. D. Taylor, M. Merlo, R. Pegleya, and M.P. Cavatorta, The Effect of Stress Concentrations on the Fracture Strength of Olymethylmethacrylate, *Mater. Sci. Eng. A*, 2004, **382**, p 288–294
18. W. Loyens and G. Groeninckx, Deformation Mechanisms in Rubber Toughened Semicrystalline Polyethylene Terephthalate, *Polymer*, 2003, **44**, p 4929–4941
19. C.B. Bucknall, I. Partridge, and M.V. Ward, Rubber Toughening of Plastics, *J. Mater. Sci.*, 1984, **19**, p 2064–2082
20. O. Julien, Ph. Begulin, I. Monnerie, and H.-H. Kausch, Loading-Rate Dependence of the Fracture Behaviour of Rubber-Modified Poly(Methyl Methacrylate), *Toughened Plastics II: Novel Approaches in Science & Engineering*, C. Keith Riew and Anthony J. Kinloch, Eds., Advances in Chemistry Series 252, American Chemical Society, 1996, p 233–252
21. A. Savadori, Methods of Measurements and Interpretation of results, in *Rubber Toughened Engineering Plastics*, A.A. Collyar, ed. Chapman & Hall, London, 1994, pp. 90–135
22. R.W. Truss and G.A. Chadwick, Tensile Behaviour of ABS Polymers, *J. Mater. Sci.*, 1976, **11**, p 111–117
23. David Broek, *Elementary Engineering Fracture Mechanics*, Martinus Nijhoff Publishers, Dordrecht, 1986
24. D.R. Askeland and P.P. Phulé, *The Science and Engineering of Materials*, 4th ed., Brooks Cole Publishing, a division of Thomson Learning, 2004
25. R.J. Young and P.A. Lovell, *Introduction to Polymers*. 2nd ed., CHAPMAN & HALL, London, 1991
26. J. Marin, *Testing of Polymers*, Vol.1, John V. Schmitz, Ed., John Willey & Sons, Inc., New York, 1965, p 87
27. C.R. Brooks and A. Choudhury, *Failure Analysis of Engineering Materials*. McGraw-Hill Companies, New York, 2002